erence is substantial, then the protonated intermediate cannot readily pseudorotate, since a pseudorotation would place the protonated oxygen atom in an equatorial position. Even if these considerations are not binding, the concentrations of the protonated species may be too low to permit it to serve as an intermediate for pseudorotation.

The kinetic equation that corresponds to (3) is

$$\frac{-\mathrm{d(ester)}}{\mathrm{d}t} = \frac{k_1k_2k_3K(\mathrm{ester})(\mathrm{H}^+)}{k_{-1}k_2(\mathrm{H}^+) + k_{-1}k_{-2}K' + k_2k_3K} = k_{\mathrm{obsd}}(\mathrm{ester}) \quad (4)$$

The only differences between the acidity of **10** and **11**, or their rates of decomposition, are probably statistical, so as a good first approximation, $k_{-1} = k_3$, $k_{-2} = 2k_2$, and $K' = 2K$, so that

$$k_{\mathrm{obsd}} = \frac{\frac{1}{5}k_1(\mathrm{H}^+)}{\frac{k_3(\mathrm{H}^+)}{5k_2K} + 1} \quad (5)$$

The kinetic equations (4 -5) show that, at low hydrogen ion concentration, the rate is proportional to acidity, but at high hydrogen ion concentration, the rate becomes independent of acidity. Experimentally, the rate for the dimer becomes more or less independent of acidity in the region from pH 1 to 0. In stronger acid, the rate is lower. This decrease in rate at high acidity is a salt effect of the type previously[25-27] discussed; the data of Table II show that the rate is decreased by large concentrations of sodium perchlorate as much as by large concentrations of acid. However, the rate maximum at 0.05–0.2 *M* acid is unlikely to be caused by a salt effect and has therefore to be ascribed to rate-limiting pseudorotation.

Rate Constant for Pseudorotation. The data in hand are insufficient to estimate the rate constant for pseudorotation. Although we might estimate that k_{-1} or k_3 has the maximum value permitted[31] in solution of about 10^{10} sec^{-1}, we cannot at present estimate K, the ionization constant for a protonated oxyphosphorane. The ionization constants are known[27] for the protonation of some esters of tetracovalent phosphorus acids, but the alkoxy derivatives of pentacovalent phosphorus are insufficiently stable to permit a determination or estimation of the ionization constants of the conjugate acids. Without such constants, the rate for pseudorotation cannot be estimated directly.

Acknowledgments. The authors are indebted to the National Science Foundation for a grant (GP-6465X) for the support of this work, and to the National Institutes of General Medical Sciences of the National Institutes of Health for a predoctoral fellowship for R. K. We also wish to thank Mr. Hampar Janjigian for his skilled technical assistance with the nmr experiments that involve decoupling.

---

[31] M. Eigen, *Angew. Chem. Intern. Ed. Engl.*, **3**, 1 (1964).

The Molecular and Crystal Structure of $P_2O_4C_{12}H_{18}$, 1,8-Diethoxy-3a,4,7,7a-tetrahydro-4,7-phosphinidenephosphindiole 1,8-Dioxide. A Diels–Alder Dimer of 1-Ethoxyphosphole 1-Oxide

Yuan-yuan H. Chiu and William N. Lipscomb

Contribution from the Department of Chemistry, Harvard University, Cambridge, Massachusetts 02138. Received January 13, 1969

Abstract: The molecular structure of a compound $P_2O_4C_{12}H_{18}$ shows a tricyclic system, in agreement with the chemical evidence. In addition, the ring juncture is shown to be *endo*, and the stereochemistry of O atoms and O–C_2H_5 units at the P atoms is established. The P atom at the bridge has a C–P–C angle of 87°, strained considerably more than that of 96° in the *endo*-fused ring. The higher hydrolytic reactivity of this bridge P atom has been associated with this additional strain by Westheimer and his associates, who have proposed a transition state in detail for the reaction at the P atoms of this and related molecules. The unit cell is orthorhombic, and there are four molecules in the unit cell of dimensions $a = 12.61$, $b = 15.30$, and $c = 7.24$ Å. The space group is Pba2, and the data taken at $-40°$ yield a value of $R = \Sigma||F_o| - |F_c||/\Sigma|F_o| = 0.10$ for the 846 independent X-ray maxima.

Westheimer[1] and his associates have shown that the rate of hydrolysis of five-membered cyclic phosphate esters, *e.g.*, methyl ethylene phosphate, is greater by over a millionfold than the rate of hydrolysis of trimethyl phosphate. This enhancement of rate applies both to ring opening and to hydrolysis of the ester group external to the ring.[2-4] This latter hydrolysis is elegantly conceived[4] to lead to a trigonal-bipyramidal transition state, which diminishes strain in the five-membered ring by accommodating a near 90° O (apical)–P–O (equatorial) angle in the ring, and which is followed

---

[1] F. H. Westheimer, *Accounts Chem. Res.*, **1**, 70 (1968).

[2] P. C. Haake and F. H. Westheimer, *J. Am. Chem. Soc.*, **83**, 1102 (1961).

[3] F. Covitz and F. H. Westheimer, *ibid.*, **85**, 1773 (1963).

[4] E. A. Dennis and F. H. Westheimer, *ibid.*, **88**, 3431, 3432 (1966).

by a "pseudorotation"[4,5] to another trigonal-bipyramidal intermediate. When other alternatives are possible, the trigonal-bipyramidal intermediate in which the alkyl group is in the apical position is not favored.[4,6] However, when this alternative is the only one, as it is for the simple five-membered cyclic phosphinate esters, no enhancement of hydrolysis rates[4,7] is shown relative to those for the acyclic analogs.

However, placement of the alkyl group in the apical position of the intermediate has been suggested[8] to lead to enhanced rates when an especially large diminution of ring strain occurs in the formation of the intermediate. The synthesis of several such compounds highly strained at a C–P–C angle has now been carried out,[9,10] and the kinetics[9] do show the predicted enhancement of rates of hydrolysis. This X-ray diffraction study was carried out in order to determine the detailed stereochemistry of one of these highly strained esters, a substituted 7-ethoxy-7-phosphabicycloheptene 7-oxide[9] (Figure 1). In particular, we have established that the ring juncture has the *endo* rather than the *exo* configuration, and we have determined the stereochemistry of the substituents on the phosphorus atoms. It is to be emphasized that both of these aspects of stereochemistry were regarded as uncertain in the synthesis,[9] and that the molecular conformation described below is fully consistent with the interpretation[8] of rate data, including the suggestion[8] that the C_7–P_1–C_{12} angle, which we find to be 87°, is unusually highly strained. This angle may be compared with the O_2–P_1–O_3 bond angle of 99° previously reported[11] for methyl ethylene phosphate, and here revised to 98° as a result of further refinement (Appendix).

Structure Determination

Room Temperature Study. Although the final refinements were made on data obtained at low temperature as described below, the structure determination was carried out on a complete set of data obtained at room temperature on the Buerger automated X-ray diffractometer. The highly hygroscopic single crystals, plate-like in shape, were sealed into Spandau glass capillaries 0.5 mm in diameter inside a drybox. Preliminary photographic X-ray diffraction data indicated the absence of *h0l* reflections when *h* is odd and of *0kl* reflections when *k* is odd. Of the probable space groups, Pba2 and Pbam, the latter is eliminated by the fact that a reasonable density required only four molecules per unit cell, but with no expected molecular symmetry. Weissenberg photographs on which Al lines were superimposed for calibration led to unit cell dimensions of $a = 12.61 \pm 0.02$, $b = 15.30 \pm 0.02$, and $c = 7.24 \pm 0.01$ Å. The calculated density of 1.37 g/cm³ is in the expected range for the chemical composition, but the reactivity of the compound precluded a direct measurement of the density.

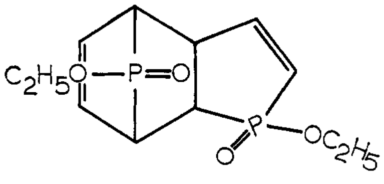

Figure 1. The chemical formula.

Furthermore, at room temperature the crystals showed noticeable intensity changes after about 2 days of X-ray exposure to Ni-filtered Cu Kα radiation. Hence, a total of eight crystals was used in the collection of some 1050 nonzero and independent X-ray diffraction maxima, including levels *hKl* for $0 \leqslant K \leqslant 15$, *0kl*, *1kl*, *hk0*, and *hk1*. After corrections for absorption,[12] Lorentz, and polarization factors the data were correlated by least-squares procedures in which the function[13]

$$R = \sum_{hi,hj} w_{hij}(\ln s_i I_{hi} - \ln s_j I_{hj})^2$$

was minimized. Here, s_i is the scale factor for the *i*th set, I_{hi} is the intensity of reflection *h* in the *i*th set, $w_{hij} = (\sigma_{hi}^2 + \sigma_{hj}^2)^{-1}$, and σ_{hi} is the statistical error in I_{hi}. The correlation factor

$$R_c = \frac{\sum_h |I_{hi} - I_{hj}|}{\sum_h |I_{hi} + I_{hj}|}$$

is 0.098 for these data.

The positions of the two phosphorus atoms were found from an analysis of the three-dimensional Patterson function. Initial phases, computed from these phosphorus atoms, followed by successive refinements of three-dimensional electron density maps then led to the discovery of all atoms of the molecule, except that C_{17} and C_{18} had to be assigned to two relatively weak and ill-defined peaks which were in chemically reasonable positions. However, the *endo* conformation of the molecule was clearly established.

Further refinement of the room-temperature structure proceeded reasonably satisfactorily. Starting from isotropic thermal parameters, $B = 4.0$ Å², for all atoms and a value of $R = \Sigma||F_o| - |F_c||/\Sigma|F_o|$ of 0.33, the least-squares method yielded a value of $R = 0.21$ after several cycles of refinement of all scale, positional, and isotropic thermal parameters. Fractional weights, $w = 1/|F_o|^2$, were employed in minimizing the quantity $\Sigma w(|F_o|^2 - |F_c|^2)^2$. However, C_{13} and C_{18} refined to isotropic thermal parameters of 12 Å² and 20 Å², respectively, and the bond distance C_{13}–C_{18} was only 1.00 Å. A three-dimensional difference electron density map from which only C_{13} and C_{18} were omitted in the calculated amplitudes suggested that the ethyl group was disordered. In our most reasonable atomic interpretation of this sausage-shaped region, which was elongated along the crystallographic *z* axis, we placed (statistically) one-half of each C atom of this ethyl group into this difference density. After verifying that this region disappeared when a new difference map was

---

(5) R. S. Berry, *J. Chem. Phys.*, **32**, 933 (1960).

(6) E. L. Muetterties, W. Mahler, and R. Schmutzler, *Inorg. Chem.*, **2**, 613 (1963).

(7) G. Aksnes and K. Bergesen, *Acta Chem. Scand.*, **20**, 2508 (1966).

(8) R. Kluger, F. Kerst, D. G. Lee, E. A. Dennis, and F. H. Westheimer, *J. Am. Chem. Soc.*, **89**, 3918 (1967).

(9) R. Kluger, F. Kerst, D. G. Lee, and F. H. Westheimer, *ibid.*, **89**, 3919 (1967).

(10) D. Samuel and B. L. Silver, *Advan. Phys. Org. Chem.*, **3**, 123 (1965).

(11) T. A. Steitz and W. N. Lipscomb, *J. Am. Chem. Soc.*, **87**, 2488 (1965).

(12) T. C. Furnas, "Single Crystal Orienter Instruction Manual," General Electric Company, Milwaukee, Wis., 1957.

(13) (a) P. G. Simpson, Ph.D. Thesis, Harvard University, 1963; (b) A. D. Rae, *Acta Cryst.*, **19**, 683 (1965); (c) A. D. Rae and A. B. Blake, *ibid.*, **20**, 586 (1966).

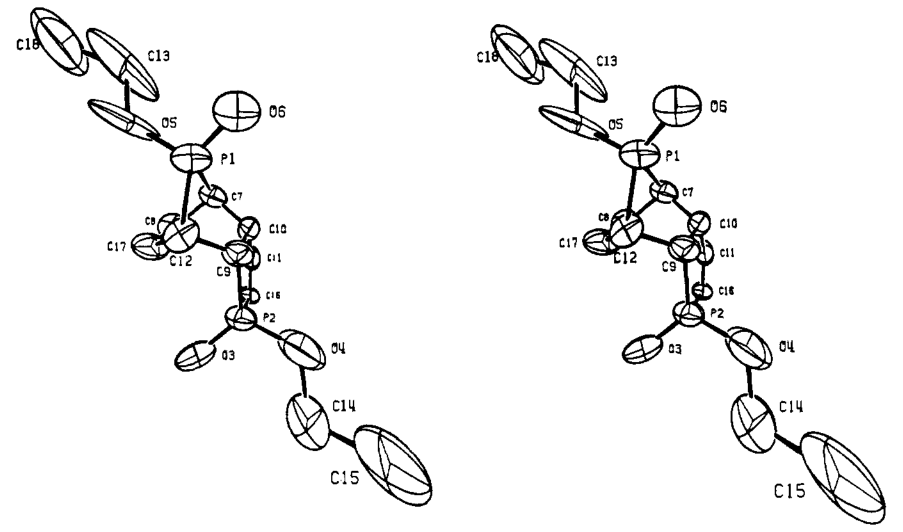

Figure 2. Stereoview of the dimer of 1-ethoxyphosphole 1-oxide.

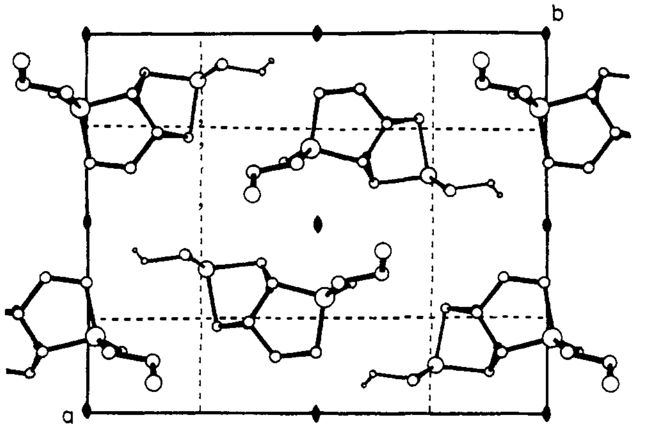

Figure 3. Packing diagram in a unit cell projected along *z* axis.

computed, including contributions of these half-atoms, we then assigned isotropic thermal parameters of 10 Å^2 to each of these four half-atoms and refined the remainder of the atomic positions in the molecule with the use of anisotropic thermal parameters. The lowest value of R thus obtained was 0.14, but slight shifts of the half-atoms of the disordered ethyl group produced fluctuations in bond distances and angles in the remainder of the molecule. The very large standard deviations of final distances and angles are partly to be associated with the rapid decline of intensities, such that for $2\theta \geqslant 100°$ the errors were so large those intensities were not included in these refinements.

Low-Temperature Study. At this stage, the data were recollected photographically in an apparatus in which the crystal was maintained at −30 to −45° in a stream of N_2, in an attempt to remove the large thermal fluctuations or disorder of the ethyl group. A crystal, 0.38 × 0.36 × 0.18 mm in dimensions, yielded Weissenberg levels *Hkl* for $0 \leqslant H \leqslant 6$, and a crystal, 0.28 × 0.16 × 0.08 mm, yielded levels *hKl* for $0 \leqslant K \leqslant 5$. Absorption corrections were made based on accurately measured crystal dimensions, and, after the usual Lorentz and polarization corrections, the data were correlated to a final list including 806 independent observed reflections and 40 nonobserved reflections which were used[14] in the refinement. A difference electron density map from which the two ethoxy groups had been omitted yielded six unambiguous peaks for these atoms. Refinement of scale, positional, and isotropic thermal parameters for all atoms (except hydrogen) reduced R to 0.17 for the 846 independent reflections. In these refinements the quantity $\Sigma w(|F_o|^2 - |F_c|^2)^2$ was minimized, where $w = 1/|F_o|^2$ for all $|F_o| \geqslant 4.0$, and $w = 4^{-1}|F_o|^{-1}$ for $|F_o| \leqslant 4.0$. After further refinement with the use of anisotropic thermal parameters the value of R became 0.102, and the weighted R_w became $R_w = \Sigma w(|F_o|^2 - |F_c|^2)^2/\Sigma w|F_o|^4 = 0.035$ for the 846 reflections.

Results and Discussion

The considerable improvement in the accuracy of the structure determination at −40°, and the lowered rate of decomposition of the material by the X-ray beam, recommend the use of this technique when mild disorder is present in the crystal structure.

The molecular configuration (Figure 2) is shown as a stereoview of one of the enantiomers: the synthesis presumably results in a racemic mixture. Details of molecular packing, summarized in Figure 3, show no abnormal van der Waals contacts between different molecules. The packing does, however, reveal some features which are associated with the disordered nature of the ethyl group C(13)–C(18). The five molecules surrounding this group are related by (1) translation by $-c$, (2) glide along b, (3) glide along b and translation by $-c$, (4) glide along $-a$, and (5) glide along $-a$ and translation by $-c$. The distance of 3.5 Å from the methylene carbon C(13) to C(16)′ of the second neighboring molecule does not allow much freedom of motion in this direction, but the distances from C(13) to nearest atoms of the other four molecules in the range from 4.4 to 5.2 Å are much larger than the van der Waals contact of about 3.6 to 4.0 Å. The methyl carbon C(18) has a neighbor, C′(16), only 3.6 Å away in class 3 above, and is 3.6 Å from O′(6) in class 1 above, but the

---

[14] Of the 221 reflections which were below the observational limits which were appropriate to the region of sin θ and α_1, α_2 splitting, those 40 for which the calculated value of the intensity exceeded the appropriate limit were included in the least-squares analysis.

other distances are in the range from 4.2 to 5.0 Å. Thus there is ample room for disorder of this ethyl group, and the intermolecular contacts suggest that this disorder should be anisotropic. Positional parameters (Table I), bond distances (Table II), bond angles (Table III), thermal parameters (Table IV), and analysis of calculated and observed structure factor disagreement (Table V) are also presented.[15]

Table I. Final Positional Parameters of the Molecule with Standard Deviations in Parentheses

Atoms	*X/A*	*Y/B*	*Z/C*
P(1)	0.1227 (5)	0.2428 (3)	0.3218[a]
P(2)	0.1969 (5)	−0.0147 (3)	0.4907 (15)
O(3)	0.1605 (12)	−0.0731 (7)	0.3424 (29)
O(4)	0.1578 (21)	−0.0453 (9)	0.6962 (27)
O(5)	0.0871 (18)	0.2848 (7)	0.1341 (28)
O(6)	0.0837 (16)	0.2909 (10)	0.4740 (35)
C(7)	0.2739 (20)	0.2207 (11)	0.3311 (38)
C(8)	0.2705 (21)	0.1534 (17)	0.1497 (38)
C(9)	0.1597 (17)	0.0988 (11)	0.4785 (38)
C(10)	0.2625 (19)	0.1518 (12)	0.4986 (39)
C(11)	0.3551 (16)	0.0932 (13)	0.5053 (33)
C(12)	0.1053 (12)	0.1239 (11)	0.3086 (41)
C(13)	0.1030 (29)	0.3792 (17)	0.0980 (50)
C(14)	0.1333 (27)	−0.1395 (20)	0.7192 (46)
C(15)	0.0746 (23)	−0.1417 (25)	0.8939 (49)
C(16)	0.3426 (15)	0.0044 (9)	0.5044 (33)
C(17)	0.1757 (23)	0.1072 (13)	0.1404 (35)
C(18)	0.0716 (26)	0.3986 (20)	−0.0805 (42)

[a] The value of this coordinate was chosen as a constant in order to define the origin along the *z* axis of the unit cell.

Table II. Bond Distances (Å) in the Molecule with Standard Deviations[a] in Parentheses

Bonds	Distances	Bonds	Distances
P(1)—O(5)	1.57 (2)	C(7)—C(8)	1.67 (4)
P(1)═O(6)	1.41 (2)	C(7)—C(10)	1.61 (3)
P(1)—C(7)	1.94 (3)	C(8)═C(17)	1.39 (4)
P(1)—C(12)	1.84 (2)	C(9)—C(10)	1.54 (3)
P(2)═O(3)	1.47 (2)	C(9)—C(12)	1.46 (4)
P(2)—O(4)	1.64 (2)	C(10)—C(11)	1.47 (3)
P(2)—C(9)	1.80 (2)	C(11)═C(16)	1.37 (2)
P(2)—C(16)	1.86 (2)	C(12)—C(17)	1.53 (4)
O(4)—C(14)	1.48 (3)	C(13)—C(18)	1.39 (5)
O(5)—C(13)	1.48 (3)	C(14)—C(15)	1.47 (5)

[a] Standard deviations were calculated from the errors of atomic coordinates.

Table III. Bond Angles in the Molecule with Standard Deviations[a] in Parentheses

Angles	Degrees	Angles	Degrees
O(5)-P(1)-O(6)	111.3 (1.1)	C(8)-C(7)-C(10)	100.7 (1.5)
O(5)-P(1)-C(7)	112.5 (1.2)	C(7)-C(8)-C(17)	111.9 (2.1)
O(5)-P(1)-C(12)	109.1 (1.0)	P(2)-C(9)-C(10)	106.5 (1.4)
O(6)-P(1)-C(7)	113.9 (1.2)	P(2)-C(9)-C(12)	114.6 (1.6)
O(6)-P(1)-C(12)	121.0 (1.1)	C(10)-C(9)-C(12)	109.8 (1.6)
C(7)-P(1)-C(12)	86.9 (0.7)	C(7)-C(10)-C(9)	110.4 (2.0)
O(3)-P(2)-O(4)	113.3 (1.0)	C(7)-C(10)-C(11)	110.7 (2.0)
O(3)-P(2)-C(9)	118.0 (1.1)	C(9)-C(10)-C(11)	110.5 (1.5)
O(3)-P(2)-C(16)	116.2 (1.0)	C(10)-C(11)-C(16)	120.9 (1.8)
O(4)-P(2)-C(9)	104.0 (1.1)	P(1)-C(12)-C(9)	99.2 (1.4)
O(4)-P(2)-C(16)	107.1 (1.2)	P(1)-C(12)-C(17)	97.9 (1.3)
C(9)-P(2)-C(16)	96.2 (0.8)	C(9)-C(12)-C(17)	110.8 (1.7)
P(2)-O(4)-C(14)	116.3 (1.7)	O(5)-C(13)-C(18)	109.6 (2.6)
P(1)-O(5)-C(13)	120.9 (1.8)	O(4)-C(14)-C(15)	103.0 (2.6)
P(1)-C(7)-C(8)	93.2 (1.5)	P(2)-C(16)-C(11)	105.6 (1.3)
P(1)-C(7)-C(10)	93.0 (1.5)	C(8)-C(17)-C(12)	112.1 (2.0)

[a] Standard deviations were calculated from the errors in atomic coordinates.

The geometrical aspects of greatest interest are the *endo*, rather than the *exo*, configuration of the molecule and the configurations of the terminal oxygen and ethoxy groups at each of the two P atoms. Neither of these two aspects of stereochemistry were established by the chemical and physical studies so far available.[9] The abnormally great strain at the bridge P(1), predicted in the study[8] of kinetics, is indicated by the C_7–P_1–C_{12} bond angle of 87°, which is about 20° less than the tetrahedral angle and indicates many times the strain energy exhibited by the C_9–P_2–C_{16} bond angle of 96°, because of the increased steepness of the expected potential function as the distortion increases. Also, the five-membered ring containing P_2 is planar within the rather large experimental errors. Other bond angles which are considerably less than tetrahedral are P_1–C_7–C_8 = 93°, P_1–C_7–C_{10} = 93°, P_1–C_{12}–C_9 = 99°, and P_1–C_{12}–C_{17} = 98°. It is rather easier to ascribe some significance to these angle strains, which are very large when compared to the standard deviations of about 2°, than it is to the distances. Thus we cannot be sure that the larger P_1–C_7 = 1.94 Å and P_1–C_{12} = 1.84 Å distances are truly significantly larger than the P_2–C_9 = 1.80 Å and P_2–C_{16} = 1.86 Å, even though standard deviations are 0.02 to 0.03 Å, since the variations of these distances for nearly equivalent bond types seem so large. Also, the distances C_7–C_8 = 1.67 Å, C_7–C_{10} = 1.61 Å, and C_9–C_{12} = 1.46 Å distorted beyond normal acceptable ranges of bond lengths are suspect, but the thermal disorder of the ethyl group could explain the abnormally short C_{13}–C_{18} distance.

Even though the precision and accuracy of this thermally disordered crystal structure are somewhat low, in spite of our efforts to lessen the difficulty by retaking all data at −40°, we feel that the major object of the study has been achieved. The stereochemistry has been established with certainty, and the large strains in bond angles anticipated by the chemical study have a quantitative basis. The structure is fully compatible with the results of the kinetic studies.

Acknowledgment. We thank F. H. Westheimer for suggesting that we undertake this study, R. Kluger and F. H. Westheimer for the material, J. A. Hartsuck for frequent and helpful advice, R. E. Marsh and G. N. Reeke, Jr., for their crystallographic program system (CRYRM), and the National Institutes of Health for financial support.

---

[15] The complete list of observed and calculated structure factors has been deposited as Document No. NAPS-00445 with the ASIS National Auxiliary Publication Service, c/o CCM Information Sciences, Inc., 22 West 34th St., New York, N. Y. 10001. A copy may be secured by citing the document number and remitting $1.00 for microfiche or $3.00 for photocopies. Advance payment is required. Make checks or money orders payable to: ASIS-NAPS.

Table IV. Final Thermal Parameters Expressed as $\exp[-(\beta_{11}h^2 + \beta_{22}k^2 + \beta_{33}l^2 + \beta_{12}hk + \beta_{13}hl + \beta_{23}kl)]$ with Standard Deviations in Parentheses

Atoms	β_{11}	β_{22}	β_{33}	β_{12}	β_{13}	β_{23}
P(1)	0.0077 (4)	0.0033 (2)	0.0325 (15)	0.0011 (6)	−0.0034 (18)	−0.0010 (13)
P(2)	0.0075 (5)	0.0032 (2)	0.0273 (12)	0.0002 (5)	0.0028 (19)	0.0012 (11)
O(3)	0.0099 (15)	0.0030 (5)	0.0341 (42)	0.0014 (14)	−0.0052 (49)	−0.0070 (28)
O(4)	0.0271 (35)	0.0045 (7)	0.0362 (52)	−0.0028 (25)	0.0255 (69)	0.0028 (33)
O(5)	0.0211 (25)	0.0021 (5)	0.0452 (55)	0.0010 (18)	−0.0327 (66)	0.0074 (28)
O(6)	0.0119 (16)	0.0079 (8)	0.0368 (49)	0.0101 (23)	0.0007 (65)	0.0031 (43)
C(7)	0.0136 (24)	0.0046 (9)	0.0285 (54)	0.0042 (26)	−0.0025 (84)	0.0048 (46)
C(8)	0.0058 (19)	0.0071 (13)	0.0348 (66)	0.0034 (32)	−0.0050 (63)	0.0020 (54)
C(9)	0.0069 (16)	0.0034 (7)	0.0250 (52)	−0.0036 (21)	0.0030 (69)	−0.0000 (40)
C(10)	0.0125 (23)	0.0049 (8)	0.0165 (36)	0.0058 (26)	0.0001 (69)	−0.0002 (46)
C(11)	0.0092 (18)	0.0064 (10)	0.0166 (42)	0.0034 (25)	0.0035 (64)	0.0029 (42)
C(12)	0.0026 (10)	0.0055 (9)	0.0281 (55)	0.0057 (20)	0.0040 (53)	0.0008 (47)
C(13)	0.0212 (46)	0.0069 (14)	0.0576 (123)	−0.0104 (42)	−0.0314 (119)	0.0261 (69)
C(14)	0.0209 (43)	0.0078 (17)	0.0325 (80)	−0.0056 (47)	−0.0084 (99)	0.0071 (59)
C(15)	0.0114 (27)	0.0155 (26)	0.0423 (98)	−0.0105 (53)	0.0102 (88)	0.0205 (79)
C(16)	0.0098 (17)	0.0023 (5)	0.0190 (39)	0.0034 (18)	0.0016 (62)	0.0026 (32)
C(17)	0.0116 (26)	0.0043 (9)	0.0275 (60)	0.0026 (28)	−0.0078 (70)	0.0050 (41)
C(18)	0.0126 (31)	0.0109 (20)	0.0370 (82)	−0.0010 (42)	−0.0010 (76)	0.0199 (66)

Table V. Analysis of Disagreement Factor R^a

Max $(\sin \theta/\lambda)^2$ in range	No. of reflections	R	Class	$R(hkl)$
0.026	33	0.07	All	0.10
0.053	47	0.08	$H = 2N$	0.09
0.079	66	0.08	$H = 2N + 1$	0.12
0.105	72	0.09	$K = 2N$	0.11
0.131	78	0.09	$K = 2N + 1$	0.10
0.158	72	0.10	$L = 2N$	0.11
0.184	80	0.10	$L = 2N + 1$	0.10
0.210	71	0.14	$K + L = 2N$	0.11
0.237	67	0.12	$K + L = 2N + 1$	0.10
0.263	60	0.15	$L + H = 2N$	0.11
0.289	51	0.20	$L + H = 2N + 1$	0.10
0.316	52	0.16	$H + K = 2N$	0.12
0.342	43	0.21	$H + K = 2N + 1$	0.10
0.368	36	0.19	$H + K + L = 2N$	0.10
0.394	18	0.33	$H + K + L = 2N + 1$	0.11

[a] $R = \Sigma||F_o| - |F_c||/\Sigma|F_o|$.

Table VI. Final Structure Parameters for Methyl Ethylene Phosphate

Atom	x	y	z
P(1)	0.2500[a]	0.0241 (4)	0.2500[a]
O(2)	0.2425 (11)	0.1787 (16)	0.3886 (10)
O(3)	0.1293 (9)	0.1219 (15)	0.1073 (11)
O(4)	0.3751 (9)	0.0899 (14)	0.2308 (13)
O(5)	0.2495 (19)	−0.2176 (13)	0.2713 (21)
C(6)	0.1261 (16)	0.3104 (27)	0.3367 (18)
C(7)	0.0682 (14)	0.3045 (23)	0.1501 (16)
C(8)	0.3944 (18)	0.3205 (29)	0.1936 (22)

[a] These coordinates were held constant to define the origin of the unit cell. Coordinates are given in fractions of unit cell.

Table VII. Bond Distances and Angles for Methyl Ethylene Phosphate

Bond	Distance, Å	Bond	Angle, deg
P(1)-O(2)	1.59 (1)	O(2)-P(1)-O(3)	98.1 (0.5)
P(1)-O(3)	1.58 (1)	O(2)-P(1)-O(4)	106.1 (0.6)
P(1)-O(4)	1.54 (1)	O(2)-P(1)-O(5)	117.7 (0.8)
P(1)-O(5)	1.45 (1)	O(3)-P(1)-O(4)	110.4 (0.6)
O(2)-C(6)	1.44 (2)	O(3)-P(1)-O(5)	115.3 (0.8)
O(3)-C(7)	1.42 (2)	O(4)-P(1)-O(5)	108.6 (0.9)
O(4)-C(8)	1.45 (2)	C(6)-O(2)-P(1)	112.4 (0.8)
C(6)-C(7)	1.56 (2)	C(7)-O(3)-P(1)	114.4 (0.8)
		C(8)-O(4)-P(1)	119.7 (1.1)
		C(7)-C(6)-O(2)	106.5 (1.2)
		C(6)-C(7)-O(3)	105.8 (1.1)

Appendix

Refinement of the Methyl Ethylene Phosphate Structure. Two further least-squares refinements of the X-ray diffraction data for methyl ethylene phosphate[11] have reduced the disagreement index R to 0.078. The weighting factors $\sqrt{w} = 1/F_o$ for $F_o \geqslant 6$, and $\sqrt{w} = 6^{-1/2}F_o^{-1/2}$ for $F_o \leqslant 6.0$ were chosen for minimization of $\Sigma w(k^2|F_o|^2 - |F_c|^2)^2$, where k is a scale factor. Final results in Tables VI (parameters), VII (distances and angles), and VIII (anisotropic thermal parameters) refer to the atom numbering of Figure 4. This numbering differs from that shown in ref 11 in the figure and text, but corresponds to that in Table I of ref 11. The interesting bond angle O_2–P_1–O_3 is 98°, changed only 1° from the 99° of the previous refinement. The large changes of bond angles, O_2–P_1–O_4 by 3° and O_3–P_1–O_4 by almost 5°, may be statistically significant in the sense that the new refinement is some improvement, but these changes do not alter the chemical conclusions. Corrections for angular oscillations which had been applied to the structure in ref 11 were not applied here.

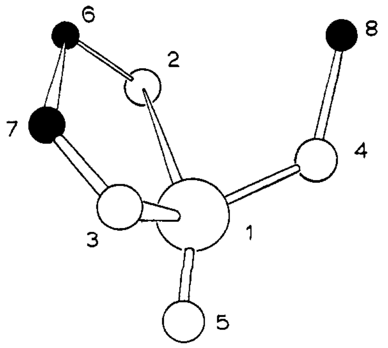

Figure 4. Structure and numbering scheme for methyl ethylene phosphate.

Table VIII. Anisotropic Temperature Factors for Methyl Ethylene Phosphate

Atom	β_{11}	β_{22}	β_{33}	β_{12}	β_{13}	β_{23}
P(1)	0.0067 (3)[a]	0.0153 (7)	0.0134 (4)	−0.001 (1)	0.0049 (5)	−0.002 (2)
O(2)	0.011 (1)	0.032 (3)	0.007 (1)	0.007 (3)	0.002 (2)	−0.001 (3)
O(3)	0.0072 (9)	0.032 (3)	0.011 (1)	0.005 (2)	0.007 (2)	−0.006 (3)
O(4)	0.0055 (9)	0.023 (3)	0.021 (2)	0.001 (2)	0.010 (2)	−0.003 (4)
O(5)	0.017 (1)	0.015 (2)	0.034 (3)	−0.007 (4)	0.021 (4)	0.001 (5)
C(6)	0.010 (1)	0.029 (5)	0.014 (2)	0.013 (4)	0.009 (3)	0.006 (5)
C(7)	0.011 (1)	0.029 (4)	0.013 (2)	0.005 (4)	0.013 (3)	0.000 (5)
C(8)	0.011 (2)	0.019 (5)	0.027 (3)	−0.002 (5)	0.019 (4)	0.005 (7)

[a] The standard deviation in the last significant figure is given in parentheses.

A special acknowledgment is due in this Appendix to K. N. Trueblood, who raised questions which led us to further refine this structure. We also acknowledge that Newton, Cox, and Bertrand[16] have already pointed out the typographical omission of the minus sign on the *y* coordinate of atom O_5.

---

(16) M. G. Newton, J. R. Cox, Jr., and J. A. Bertrand, *J. Am. Chem. Soc.*, **88**, 1503 (1966).

Molecular Conformations in Highly Crowded Molecules. Electronic Spectra of Some N-Alkyl and Poly-N-alkyl Derivatives of 1,3-Diamino-2,4,6-trinitrobenzene[1]

Richard R. Minesinger and Mortimer J. Kamlet

Contribution from the Advanced Chemistry Division, U. S. Naval Ordnance Laboratory, White Oak, Silver Spring, Maryland 20910.

Received February 12, 1969

Abstract: Absorption spectra of 1,3-diamino-2,4,6-trinitrobenzene (**3**) and its N-alkyl, N,N- and N,N′-dialkyl, and N,N,N′,N′-tetraalkyl derivatives are related to those of simpler nitro- and polynitroanilines. On the basis of spectral displacements on N-alkylation, probable preferred conformations are suggested for a number of these compounds. Spectral "band splitting" which is observed in **3** and many of its derivatives is thought to arise from electronic transitions which have parallel geometries but opposite charge displacements upon promotion to the electronic excited states. The phenomena *steric enhancement of resonance* and *electronic butressing* are shown to be operative in this series.

In earlier papers we invoked phenomena characterized as *steric enhancement of resonance*[2] and *electronic buttressing*,[3] together with more classical steric and electronic effects, to explain changes in positions and intensities of maximal absorption in the spectra of ring- and N-substituted derivatives of 2,4-dinitroaniline (**1**)[3] and 2,4,6-trinitroaniline (**2**).[4,5] Additionally, we reported attempts to deduce from these spectra some aspects of molecular conformation which had, in at least one instance,[5,6] been confirmed by a total crystal structure determination.[7] We address ourselves now to the question of how these phenomena affect spectra and conformations in the N-alkyl, N,N- and N,N′-dialkyl, and N,N,N′,N′-tetraalkyl derivatives of 1,3-diamino-2,4,6-trinitrobenzene (**3**). This series of compounds allows an interesting test of how the opposing influences of strong resonance interactions and progressively increasing substituent bulk affect coplanarity of individual substituents with the ring in highly crowded molecules.

Band Assignments for 1,3-Diamino-2,4,6-trinitrobenzene (3). With the polynitroanilines discussed earlier,[3,4] ultraviolet spectra in methanol above 250 mμ were characterized by two medium-to-high-intensity V ← N maxima (incompletely resolved in the case of **1**),[8] for which band assignments were relatively straightforward. Single medium-intensity bands, showing maxima near 400 mμ, result from *ortho* electronic interactions in 2-nitroaniline and 2,6-dinitroaniline; these positions are shifted only slightly by a variety of ring substituents. Bands of similar intensity and position of absorption (band 2) appear in the two-band systems of both **1** and **2** (Table I, Figure 1), and thus may be considered to arise from $[H_2{}^+N{=}C(1) \rightarrow C(2){=}NO_2{}^-]$ electronic transi-

---

(1) Part V in the series, "Steric Enhancement of Resonance."

(2) M. J. Kamlet, J. C. Hoffsommer, and H. G. Adolph, *J. Am. Chem. Soc.*, **84**, 3925 (1962); H. G. Adolph, B. Johnson, and M. J. Kamlet, *J. Org. Chem.*, 30, 2864 (1965).

(3) M. J. Kamlet, H. G. Adolph, and J. C. Hoffsommer, *J. Am. Chem. Soc.*, **86**, 4018 (1964).

(4) M. J. Kamlet, J. C. Hoffsommer, R. R. Minesinger, and H. G. Adolph, *J. Org. Chem.*, **33**, 3070 (1968).

(5) M. J. Kamlet, R. R. Minesinger, J. C. Hoffsommer, J. C. Dacons, and H. G. Adolph, *J. Chem. Soc.*, *B*, 1147 (1968).

(6) C. Dickinson, J. R. Holden, and M. J. Kamlet, *Proc. Chem. Soc.*, 232 (1964).

(7) C. Dickinson, J. M. Stewart, and J. R. Holden, *Acta Cryst.*, **21**, 663 (1966).

(8) Strong band overlap in **1** (Figure 1) probably shifts band 1 bathochromically and band 2 hypsochromically from their "true" positions.